A New Hunting Control Method for Permanent Magnet Hysteresis Motors

Z. Nasiri-Gheidari*, H. Lesani** and F. Tootoonchian***

Abstract: Hunting is a flutter associated with the synchronous speed that gives rise to the gyro drifting errors and may cause objectionable time-displacement errors in video head wheel drives and other precision scanning systems. In this paper, dynamic characteristics of permanent Magnet hysteresis motors are presented and hunting is explained. New damping techniques have been developed using optimized eigenvalues calculation. They are calculated from LQR optimization method. In this damping method, a distinct reduction in hunting has been archived. Furthermore field oriented control result of motor is presented that have good effect on Hunting. Nearest agreement between simulated and measurement results shows the accuracy of motor model. Comparison between this paper results and other measured damping methods result are shown its success.

Keywords: Damping Method, Dynamic Model, Field Oriented Control, Hunting, Optimal Control, Permanent Magnet Hysteresis Motor.

1 Introduction

Permenent magnet (PM) synchronous motors have several distinct advantages, namely, high efficiency, high power factor, and relatively higher stability. Smooth brushless operation and simple rotor construction of permanent magnet synchronous motors offer additional advantages particularly for high-speed applications. However, the permanent magnet synchronous motor, when operated at line frequency, has a major drawback during the starting period as the magnets generate a brake torque which decreases the starting torque and reduces the ability of the rotor to synchronize a load [1].

The hysteresis motor is widely used in small motor applications. It has not only simple constructional features with conventional polyphase stator windings and a solid rotor hysteresis ring, but also high built-in self-starting torque during the run-up and synchronization period. It has no rotor slots and thus it has low noise during operation. These advantages make the hysteresis motor especially suitable for applications, such as gyros, centrifuges, pumps, timing and recording equipment, in which constant torque, constant speed, and quiet operations are required. In spite of these advantages, the commercial hysteresis motor still suffers from chronic limitations, e.g., high magnetizing current, low power factor, and low efficiency associated with high parasitic losses [2].

The combination of permanent magnet and hysteresis materials in the rotor of the hybrid motor has many distinct advantages over the conventional PM or hysteresis motors [3], [4]. The hybrid motor in which the permanent magnets are inserted into the slots at the inner surface of the hysteresis ring is called the permanent magnet hysteresis synchronous (PMHS) motor [1].

Figure 1 shows the schematic of the hybrid PMHS motor [1]. During asynchronous speed, the motor torque consists of the hysteresis torque, eddy current torque and permanent magnet brake torque. At synchronous speed the motor torque comprises of the hysteresis and permanent magnet torques. It combines the advantageous features of both the hysteresis and permanent magnet motors. The negative affect of the magnet brake torque is compensated by the eddy current torque, particularly at the initial run up period [1]. While motor is driving a constant torque load, the rotor motion may have superimposed on its steady synchronous speed a meandering of its rotor phase angle about that of the constant-speed field vector. This excursion is usually oscillatory, with a characteristic period, but has an amplitude and phase which vary randomly. Small hysteresis synchronous motors which are used in timing and recording devices often offer the same behavior. The consequent time-displacement error

Iranian Journal of Electrical & Electronic Engineering, 2006.
* Zahra Nasiri-Gheidari is with the Department of Electrical Engineering, Sharif University of Technology, Tehran, Iran.
E-mail: Z_Nasiri@ee.sharif.edu
** Hamid Lesani is with the Department of Electrical and Computer Engineering, Tehran University, Tehran, Iran.
E-mail: Lesani@ut.ac.ir
*** Farid Tootoonchian is with the Department of Electrical Engineering, Iran University of Science and Technology, Tehran, Iran.
E-mail: Tootoonchian@iust.ac.ir.

may be objectionable in certain applications, notably, video head wheel motors [5]. So the rotor oscillations around the synchronous speed at a low frequency of 3-5 Hz are named hunting [5], which is related to mechanical mode of motor.

A new hunting suppression technique based on active and passive circuits is offered in [5]. It shows undamped motor oscillations by recovery from torque transient and absolute time displacement error. But it discusses about two phase hysteresis motor not PMHS motor.

Another method applied to a two-phase conventional hysteresis motor hunting has been offered in [6] that are based on transfer function calculation for the hunting angle with respect to a disturbance torque. Rate-feedback is used as a damping strategy. In the other words the derivative of the output signal (drag angle) is fed back and added algebraically to the actuating signal of system (load torque). Oscillations amplitude is about 1.9167 times and settling time is very shorter using this method. This method is also presented on three phase Permanent magnet hysteresis motors in this paper. But there are some major problems that are discussed in the paper. However in brief, rate-feedback on high order systems causes the use of output higher orders derivations which is impracticable. Therefore, other strategies must be used to solve the stability problem. A method proposed by Rissanen [7] shows that the stability of system is provided by the feedback of the state variables instead of the output signal and its derivations. On the other hand, much work on the steady-state analysis of hysteresis [8] have been reported which are based on the methods used to approximate the B-H loop of the hysteresis material [1]. In the dynamic analysis of such motors the eddy currents have been ignored. The motor dynamic can be also described by a set of nonlinear differential equations and linearized for small perturbations around the equilibrium point.

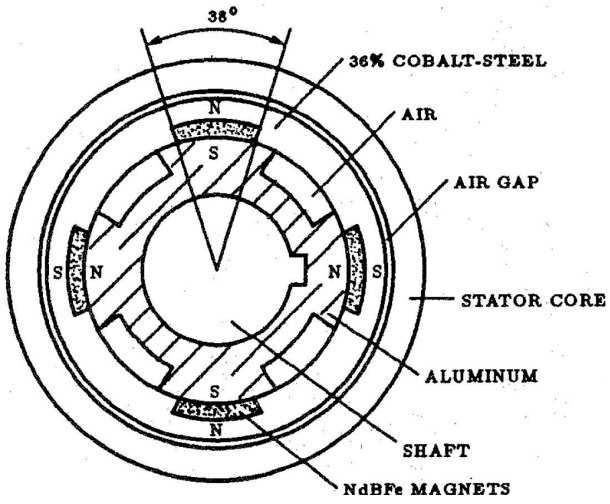

Fig. 1 Hybrid permanent magnet hysteresis motor [1].

This paper presents an approximate mathematical model to predict the dynamic of three-phase conventional hysteresis motors. Eddy current effect and its control are considered. A new hunting suppression technique based on the state feedback and optimal control theory is presented. Since selection of weighting matrix Q in the LQR design is very important, an algorithm for the selecting with the dominant eigenvalue shift is presented. Proposed method has some advantages, such as minimal overshoot and shorter settling time. Finally simulation results are compared with experimental results.

2 Motor Model

The following assumptions are considered in the analysis:

a) The stator is assumed to have a sinusoidally distributed polyphase windings [1].

b) The magnetic flux is radial in the air gap and circumferential in the rotor hysteresis material [1].

c) The hysteresis effects in the rotor hysteresis materials are taken into account in the case of both running up and synchronizing operation [9].

d) The effects of saturations is neglected [9].

e) The B-H loop of the hysteresis material is modeled by a parallelogram [1].

Figure 2 shows the model of a three phase PMHS motor [10]. Each stator winding has a leakage flux and a main flux that links the rotor. The hysteresis phenomenon in an element of the rotor ring is represented by a balanced polyphase winding, and therefore by two orthogonal closed coils, each with the same number of turns as the stator coil pair. The rotor eddy current effect is represented by the equivalent resistance R_e, which is slip dependent, and the hysteresis effect by the equivalent resistance R_h, which is slip independent [11]. The stator variables are transformed to the rotor reference frame which eliminates the time-varying inductances in the voltage equations. Park's equations are obtained by setting the speed of the stator frame equal to the rotor speed. The voltage- current equations are as shown in (1).

$$\begin{bmatrix} V_{ds} \\ V_{qs} \\ V_{dr} \\ V_{qr} \\ V_{pm} \end{bmatrix} = \begin{bmatrix} R_s + \frac{p}{\omega_b}X_{ss} & -\frac{\omega_r}{\omega_b}X_{ss} & \frac{p}{\omega_b}X_m & -\frac{\omega_r}{\omega_b}X_m & \frac{p}{\omega_b}X_m \\ \frac{\omega_r}{\omega_b}X_{ss} & R_s + \frac{p}{\omega_b}X_{ss} & \frac{\omega_r}{\omega_b}X_m & \frac{p}{\omega_b}X_m & \frac{\omega_r}{\omega_b}X_m \\ \frac{p}{\omega_b}X_{ss} & 0 & R_r + \frac{p}{\omega_b}X_{rr} & 0 & \frac{p}{\omega_b}X_m \\ 0 & \frac{p}{\omega_b}X_m & 0 & R_r + \frac{p}{\omega_b}X_{rr} & 0 \\ \frac{p}{\omega_b}X_m & 0 & \frac{p}{\omega_b}X_m & 0 & \frac{p}{\omega_b}X_m \end{bmatrix} \times \begin{bmatrix} i_{ds} & i_{qs} & i_{dr} & i_{qr} & i_{pm} \end{bmatrix}^T \quad (1)$$

The electromagnetic developed torque in a three-phase, P pole motor is given by [8]:

$$T_e = \frac{3}{2} P[(L_{ds} - L_{qs}) i_{ds} i_{qs} + L_{md} i_{dr} i_{qs} - L_{mq} i_{qr} i_{ds}] \quad (2)$$

where

$$R_r = \frac{R_e . R_h}{s R_h + R_e} \quad (3)$$

Considering parallelogram model for B-H loop of the hysteresis material, pertinent parameters R_e and R_h is obtained as [1]:

$$R_e = \frac{12 l_r . \rho}{10^4 A_h} \quad (4)$$

$$R_h = \frac{m E_g^{\ 2}}{4 B_r H_c V_r f} \quad (5)$$

where l_r is length of the rotor ring; A_h is cross-sectional area of the hysteresis ring; E_g is air-gap voltage; B_r is residual flux density of the hysteresis material; H is coercive force of the hysteresis material; V_r is volume of the hysteresis ring; ρ is specific resistivity of hysteresis material and V_{ds}, V_{qs} are d, q axis stator voltages, V_{dr}, V_{qr} are d, q axis rotor voltages, i_{ds},i_{qs} are d, q axis stator currents, i_{dr}, i_{qr} are d, q axis rotor currents, R_s, X_{ss} are resistance and reactance of stator circuit, R_r, X_{rr} are resistance and reactance of rotor circuit, L_{md} , L_{mq} are d-q axis mutual inductance between rotor and stator circuits, L_{ds}, L_{qs} are d-q axis inductance of stator, ω_b is base angular frequency, ω_r is rotor angular frequency, T_L is load torque, H is inertia constant, p is d/dt and P is number of pole pairs.

The electrical equivalent circuits of the hysteresis synchronous motor are presented in Fig. 3 [10]. $E_{\omega d}$ and $E_{\omega q}$ are as follows [10]:

$$\begin{aligned} E_{\omega d} &= (1-s)[(X_{ls} + X_m) i_{qs} + X_m i_{qr}] \\ E_{\omega q} &= (1-s)[(X_{ls} + X_m) i_{ds} + X_m i_{dr}] \end{aligned} \quad (6)$$

The linearization model will make with using perturbation method. This leads to the following linear time-invariant system of equations:

$$\begin{aligned} \dot{X} &= A X + B U \\ Y &= C X + D U \end{aligned} \quad (7)$$

where X is the n-dimensional state variable vector, U is the m-dimensional input variable vector, A is the n×n constant matrix, and B is the n×m constant matrix. The linearized equation (7) describing the first-order dynamics of small perturbation is then given in the state variable form as follows:

$$\begin{aligned} \Delta\dot{X} &= A\,\Delta X + B\,\Delta U \\ \Delta Y &= C\,\Delta X + D\,\Delta U \end{aligned} \quad (8)$$

where:

$$\begin{aligned} \Delta X &= [\Delta\psi_{qs}, \Delta\psi_{ds}, \Delta\psi'_{qr}, \Delta\psi'_{dr}, \frac{\Delta\omega_r}{\omega_b}, \Delta\delta]^t \\ \Delta U &= [\Delta V_{qs}, \Delta V_{ds}, \Delta T_{mech}]^t \\ \Delta Y &= [\Delta T_e, \Delta i_{ds}, \Delta i_{qs}, \frac{\Delta\omega_r}{\Delta\omega_b}]^t \end{aligned} \quad (9)$$

The numerical coefficients of (8) can be calculated. The eigenvalues of the open-loop system are as follows:

$$\begin{aligned} \lambda_1 &= -4.8 \\ \lambda_2 &= -6 \\ \lambda_{3,4} &= -8.2 \pm 377.1i \\ \lambda_{5,6} &= -0.8 \pm 21.9911i \end{aligned} \quad (10)$$

The first two eigenvalues belong to rotor, $\lambda_{3,4}$ are related to the stator circuit, because their frequency are close to the synchronous frequency. Finally $\lambda_{5,6}$ are the mechanical mode of system that cause the hunting oscillations with the frequency of 3.5 Hz.

System responses for standard inputs are calculated based on the above state-space equation.

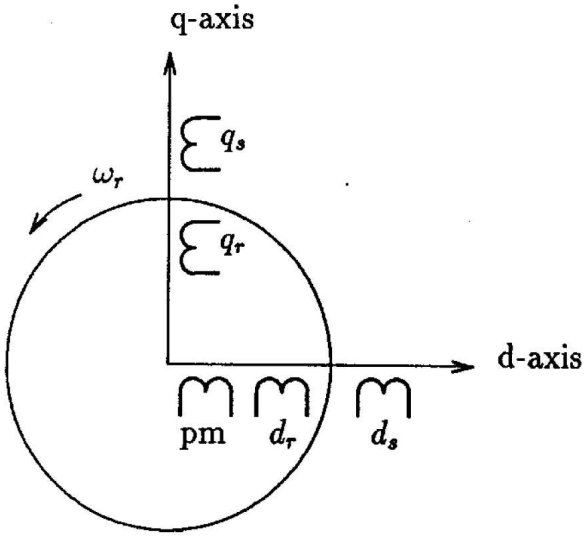

Fig. 2 d-q Axis model of PMHS motor [10].

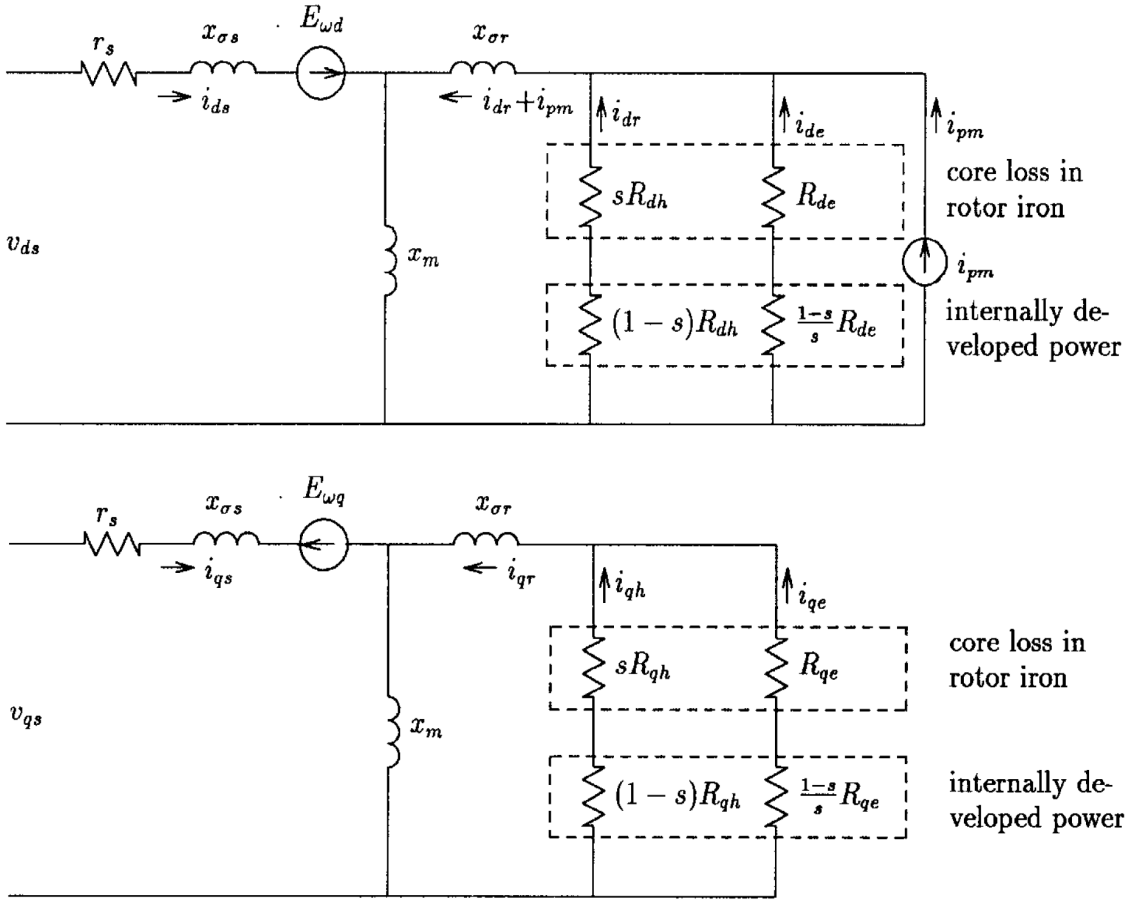

Fig. 3 Electrical equivalent circuits of the PMHS motor [10].

3 Results And Discussions

The motor has a standard three-phase, four-pole stator winding. Its ratings are 208 V, 5 hp and 60 Hz. Machine dimensions, the pertinent properties of the rotor materials and the parameters of the experimental PMHS motor are given in appendix.

Figure 4 shows the test and computed open loop speed-versus-time. Figure 4(a) and (b) shows the computed and experimental speed-versus-time responses of PMHS motor from [1] and (c) shows this paper simulation result. It is seen that the computed speed response is smoother than the experimental result. The reason is due to the difference between the cataloged and calculated areas of the hysteresis B-H loop. Because of this, it is considered that the hysteresis torque component of the computed torque is larger than the experimental result so that the computed time to reach at synchronous speed is shorter than the experimental one. The measured starting time is approximately 5.0 s and the computed time is about 4 s for [1] and 3.8 s our simulation.

Figure 5 shows the computed torque versus time during run-up and synchronizing period, from [1] and compares it with this paper result. It is seen from Fig. 5 that the pulsating torque in starting is considerable in the PMHS motor, because the PMHS motor has the pulsating torque due to both permanent magnets and magnetic saliency of the rotor.

Further, Fig. 6(a) and (b), shows the computed and experimental current-versus-time responses of PMHS motor from [1] and (c) show it, for our simulation. It can be seen that the test current not only decays more slowly, but, also, the oscillations in the test current seem to end abruptly. This reason is to predict the hysteresis torque larger than the actual one, in computing. It is considered that the computed current decays more quickly by the large hysteresis torque [1]. The difference between the test and computed results is due to the neglecting the high-frequency eddy-current effect.

Open loop step response of linearized motor model is presented in Fig. 7(a). It is very oscillatory. For damping oscillations, rate-feedback method is applied.

Compensated and uncompensated motor responses are then obtained as shown in Fig. 7. Rate feedback is proposed in [6] for a two phase conventional hysteresis motor. In [6] the transfer function is from two orders, so just output one order derivation can compensate the response. But on high order systems using of output higher orders derivations is needful, which impracticable and using derivative cause to increase interferences on the system.

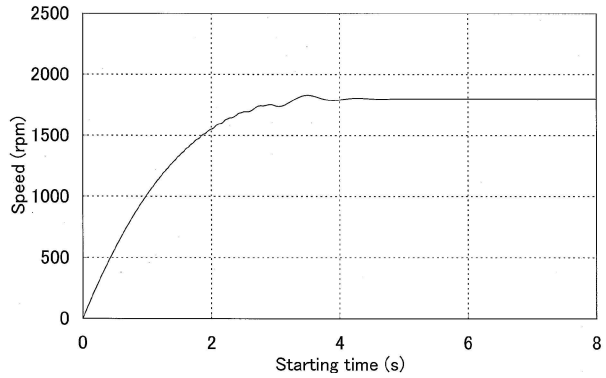

(a)

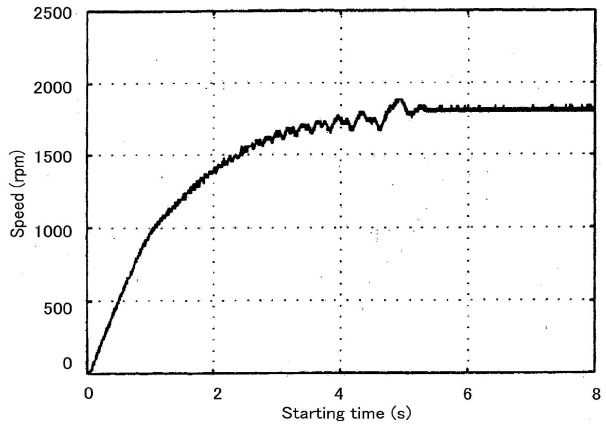

(b)

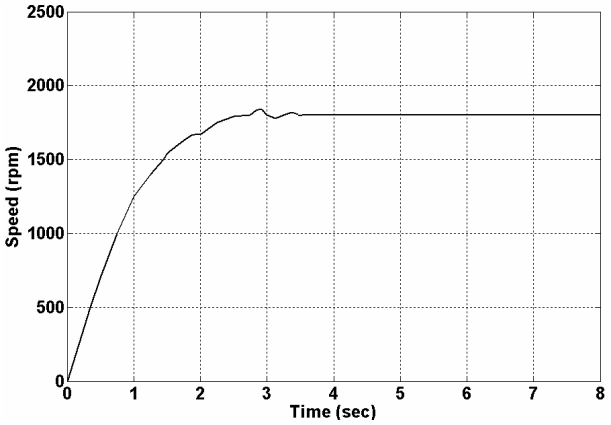

(c)

Fig. 4 Speed–time response. (a) Computed result of [1]. (b) practical test from[1], (c) This paper result.

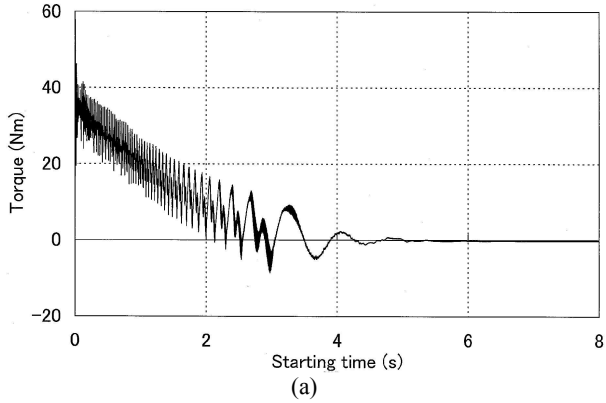

(a)

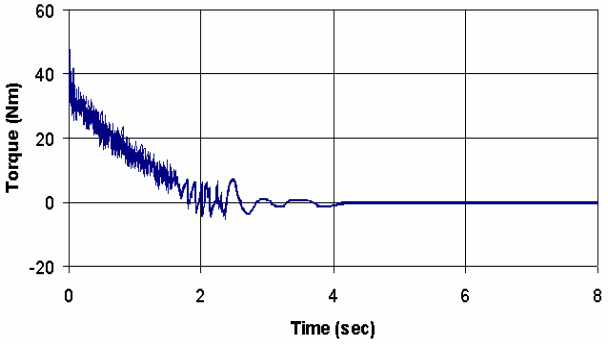

(b)

Fig. 5 Computed torque versus time (a) result of [1] (b) This paper result.

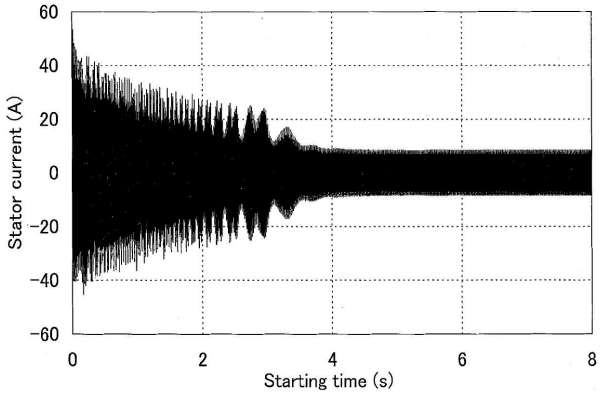

(a)

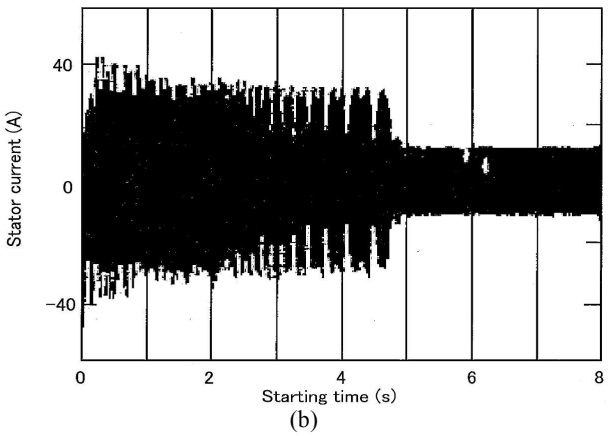

(b)

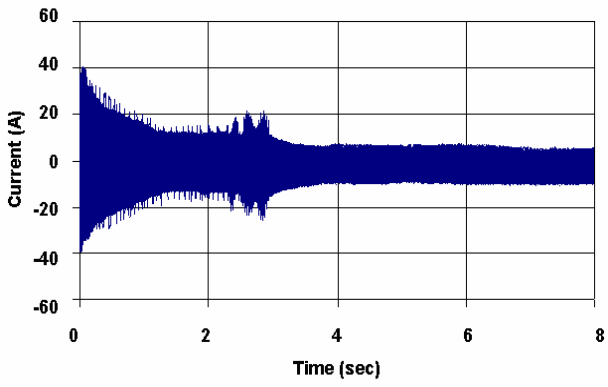

(c)

Fig. 6 Current versus time. (a) Computed result of [1]. (b) Test result of [1]. (c) This paper result.

On the other hand, comparisons between compensated and uncompensated response in Fig. 7, show this method isn't very useful. The settling time of response in open loop system is about 6 second and using rate feedback, decreases it to about 2.5 second. Other specification of response is not very good. Comparison of the compensated and uncompensated responses has been shown in Table 1.

For more compensation there are two other control techniques:

1) State feedback

2) Optimized control.

The dynamical characteristics, for example, stability, decay of oscillations or sensitivity to disturbances, are determined by the distribution of the eigenvalues of the system matrix A in the s-plane. The goal is to influence the system specifically so that it shows a desired behavior.

In this paper two methods have been compared and LQR has been applied. Before using these methods, the controllability and absorbability of the system is tested. Mechanical mode damping ratio, in open-loop system is about 0.037. Increasing the damping of system enhances the system damping but slows down the system. Assume that the desired damping ratio is about 0.3. This leads to a second order system with the following poles:

$$s_{1,2} = -\alpha \pm j\omega_d \tag{11}$$

where α and ω_d are the damping coefficient and frequency respectively and are calculated as follows:

$$\left.\begin{aligned} \alpha &= \zeta\,\omega_n \approx 6.92 \\ \omega_d &= \omega_n\sqrt{1-\zeta^2} = 21.9911 \end{aligned}\right\} \Rightarrow S_{1,2} = -6.92 \pm j\,21.9911 \tag{12}$$

If system behavior was determined with $S_{1,2}$, it is enough that other eigenvalues be in the region of insignificant poles. For this reason, real part of insignificant poles are selected at least 5 to 10 times those of a pair of complex dominant poles. So the desired eigenvalues are:

$$\begin{aligned} &\lambda_1 = -48,\ \lambda_2 = -45 \\ &\lambda_{3,4} = -50 \pm 377.1\mathrm{i} \\ &\lambda_{5,6} = -6.92 \pm 21.991\,\mathrm{li} \end{aligned} \tag{13}$$

Equation (13) shows the closed loop eigenvalues. As mentioned before, the closed-loop pole locations have a direct impact on time response characteristics such as rise time, settling time, and transient oscillations. State-space techniques uses compensator gains to move closed-loop poles to achieve design specifications. Closed loop step response by using state feedback is shown in Fig. 8. It is obvious from Fig. 8 that the state feedback method can well damp the oscillation. As shown in table I, settling time is decreased from 6 to 0.7 second and other specification can be better.

But there is a major point; pole placement can be badly conditioned if pole locations are chosen unrealistically. In particular, one should avoid placing multiple poles at the same location. Moving poles that are weakly controllable or observable, typically requires high gain, which in turn makes the entire closed-loop eigenvalue structure very sensitive to perturbations. So, pole placement technique is appropriate when one is given some desired transient performance specifications which may be directly translated into locations for the dominant closed-loop poles. For multi-input, multi-output systems, however, it is not always obvious how to interpret performance specifications in terms of pole locations. An alternative method for damping is linear quadratic regulator (LQR) algorithm. The theory of optimal control is concerned with operating a dynamic system at minimum cost.

This paper introduces a procedure for the design of modified linear-quadratic state-feedback controls. The controls improve on the known stability gain-margin properties of system. For LQR design of Permanent magnet hysteresis motor, a performance index of the quadratic form is usually chosen [12]:

$$J = \frac{1}{2}\int_0^\infty \left[x^T Q\,x + u^T R\,u\right]dt \tag{14}$$

where Q is the weighting matrix of state variable deviations and R is the control effort. The LQR is derived from the minimization of the performance index that result the following Riccati equation [12]:

$$\dot{P} = Q + PA + A^T - PRBR^{-1}B^T P = 0 \tag{15}$$

So Riccati matrix K and optimal control law can be calculated as follows:

$$\underline{U}_{opt} = -K\underline{X} \quad \text{with } K = R^{-1}B^T P \tag{16}$$

Finally the eigenvalues of the system with the LQR can be calculated from the following equations:

$$\dot{\underline{X}} = (\underline{A} - \underline{BK})\underline{X} + \underline{BU} \tag{17}$$

Since the selection of weighting matrix Q is very important in the LQR control method, it must be systematically selected. One idea is to link the selection with the left-shift of dominant eigenvalues of the motor as much as possible.

Figure 9 shows an algorithm of LQR designed [12] by selecting the weighting matrix Q with the dominant eigenvalues shift:

(a) Being with an initial weighting matrix Q:

$$Q = \text{Diag}[a \;\; b \;\; c \;\; d \;\; e \;\; j] = \text{Diag}[0 \;\; 0 \;\; 0 \;\; 0 \;\; 1 \;\; 1]$$
$$R = \text{Diag}[f \;\; g \;\; h] = \text{Diag}[1 \;\; 1 \;\; 1] \qquad (18)$$

(b) Find the new eigenvalues and Riccati matrix K.
(c) Calculate the new damping ratio.
(d) Determine whether the controller has exceeded the damping ratio limit. If not, proceed with the dominant eigenvalues shift. If yes, stop and print K of the previous stages.
(e) For the shift:

$$\lambda = \lambda + \Delta\lambda, \qquad \Delta\lambda < 0 \text{ (real)} \qquad (19)$$

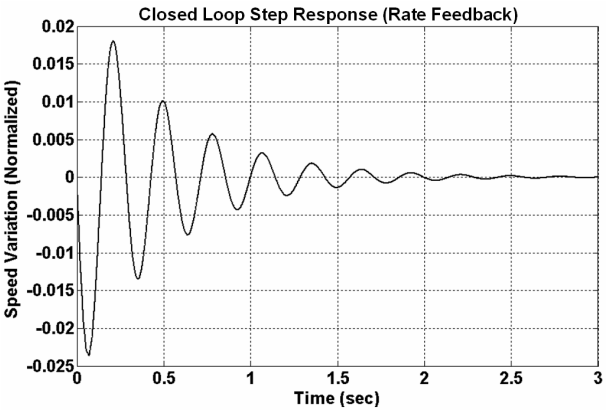

(b) rate- feedback response

Fig. 7 Comparison between open-loop with rate-feedback, speed variation response for step change in source voltage.

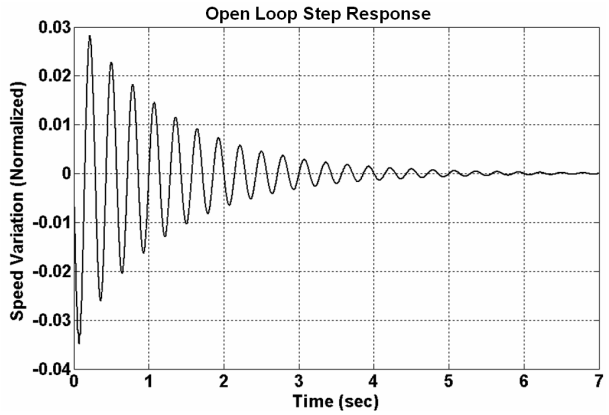

(a) Open loop response

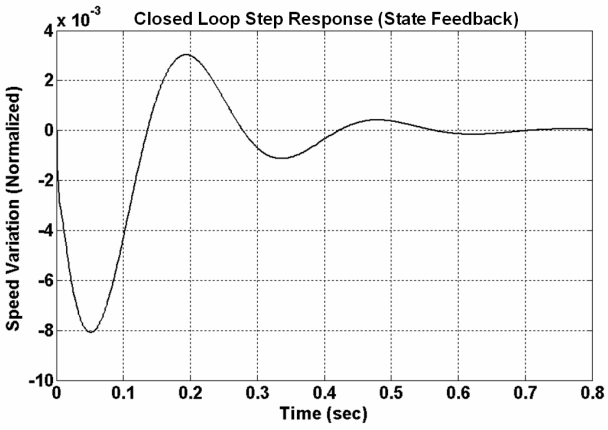

Fig. 8 Closed loop speed variations, using state feedback.

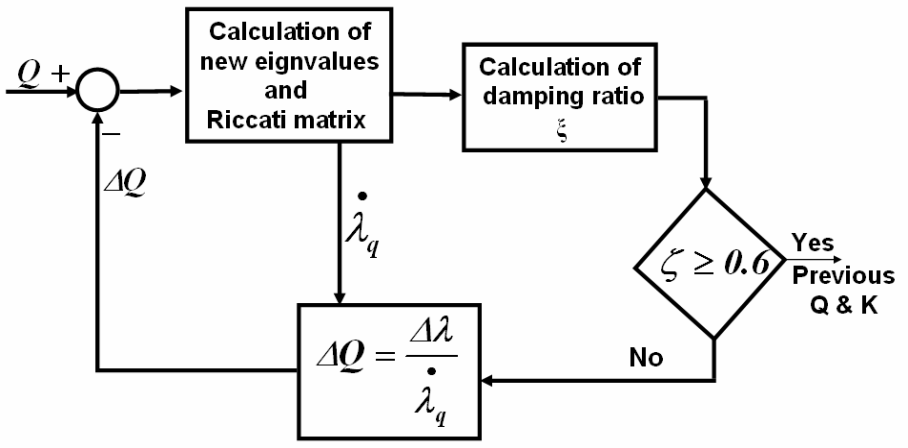

Fig.9 An algorithm of LQR design with dominant eigenvalue shift.

Each weighting matrix element is changed by small amounts and calculated from the eigenvalue sensitivity $\dot{\lambda}_q$

$$\Delta q = \Delta\lambda / \dot{\lambda}_q \qquad \Delta q < \varepsilon \qquad (20)$$

where $\dot{\lambda}_q$ is the sensitivity of the dominant eigenvalues with respect to a Q element:

$$\dot{\lambda}_q = (\partial\lambda)/\partial q \qquad (21)$$

(f) Update Q and reenter the interactive loop.
(g) Reorder the eigenvalues for the next shift.
After a dominant eigenvalues, the eigenvalues of the system will move with respect to each other, they can be then re-divided into three groups: the most dominant eigenvalues pair; the less dominant eigenvalues, some of which may have negative real parts, five to ten times the dominant ones. Only the dominant ones need be left-shifted, the movement of the rest eigenvalues shall be free [12]. Optimal Q, R and K are as follows:

$$Q = \mathrm{Diag}[0 \quad 0 \quad 0 \quad 0 \quad 10.1310 \quad 23.3902]$$
$$R = \mathrm{Diag}[1 \quad 1 \quad 1]$$
$$K = [0.8117 \quad -0.2188 \quad 0.1811 \quad -0.0890 \quad 1.0817 \quad 0.9097$$
$$0.1811 \quad -0.0497 \quad 0.1263 \quad -0.0275 \quad 0.1064 \quad 0.0198$$
$$-0.0036 \quad 0.0010 \quad -0.0004 \quad 0.0003 \quad -0.0067 \quad -0.0060]$$

Figure 10 shows the closed-loop per-unit speed variations, using LQR control, for various Q. Figure 11 shows the optimal response using the proposed algorithm in which amplitude and frequency of the hunting is largely decreased.
Operations of all the above-mentioned controllers are compared with the open-loop system in Table 1 and Fig. 12 and the optimal controller has satisfied the control objects.
The field oriented control method can be applied to the Permanent magnet hysteresis motor in order to control the hunting. In this method, the phase currents are transformed to a space vector in the stator–coordinates, and this space vector is then transformed to a dq axis in the rotor frame. The stator-to-rotor transformation depends on the actual rotor position. Therefore, the rotor position must be determined during any sampling cycle.
The drive is fed in such a way that the q-axis current provides the desired torque. Since the d-axis of the current vector points to the magnetization direction of the rotor pole, the current is suppressed by the corresponding controller.

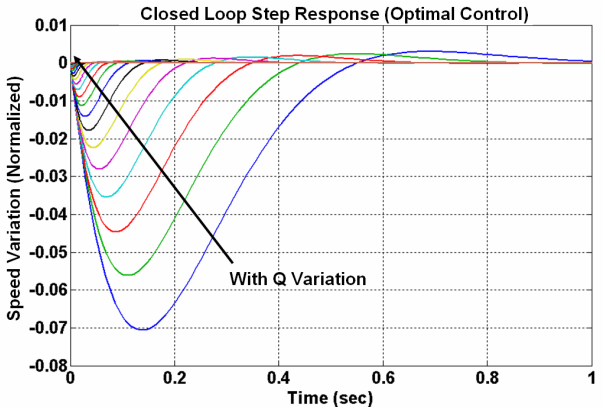

Fig. 10 Closed loop speed variations, using LQR control, for various Q.

Table 1 Comparison between controllers operation.

	Settling time (s)	Gain Margin (dB)	Phase Margin	Under shoot (p.u.)
Open loop	6	6.54	Inf.	-3.48×10^{-2}
Rate feedback	2.5	12	Inf.	-2.36×10^{-2}
State feedback	0.7	34.1	Inf.	-8×10^{-3}
Optimal controller	0.025	50.6	Inf.	-2.14×10^{-6}

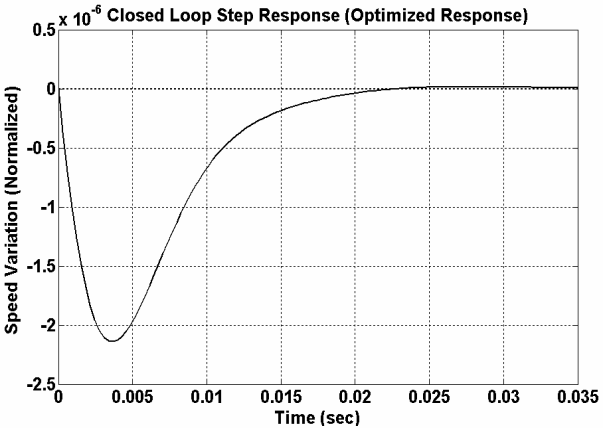

Fig. 11 Optimal response of speed variation using proposed algorithm.

Figure 13 shows the torque and speed response of motor with the step change of the load torque in which there is no hunting in the speed response. The vector control method is able to damp oscillation well, but it is complex.

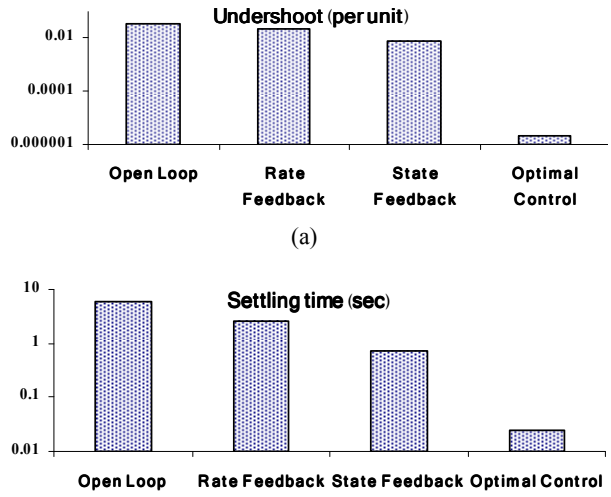

Fig. 12 Comparison of different controllers operations (a) Under shoot in per unit (b) settling time in second.

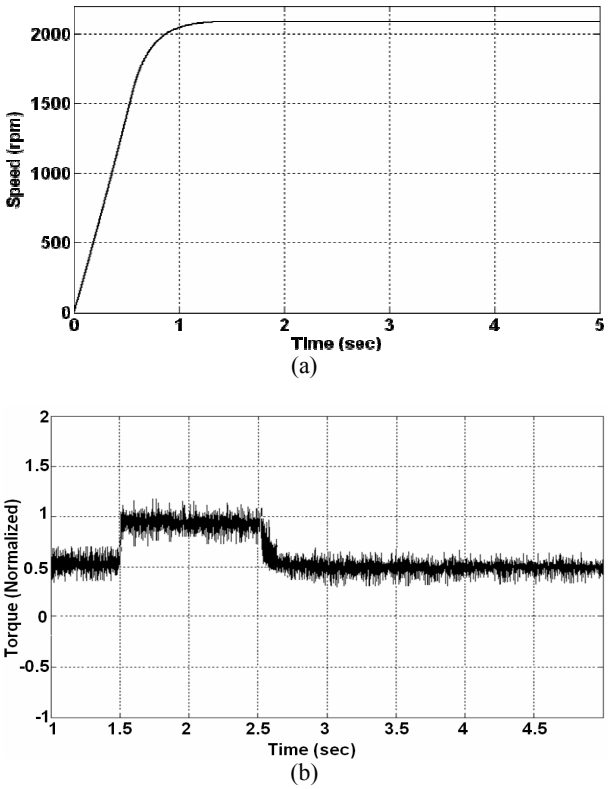

Fig. 13 Field oriented control results with step change in load torque (a) Speed versus time (b) electromagnetic torque response.

4 Conclusions

A new dynamic analysis of three-phase permanent magnet hysteresis motors has been presented by taking into account the eddy current effect. The results confirmed that the pulsating torque in starting is considerable in the PMHS motor, because the PMHS motor has the pulsating torque due to both permanent magnets and magnetic saliency of the rotor. Its dynamic responses were compared with [1] and a good agreement was achieved. Furthermore, a novel method for hunting suppression based on the state feedback and optimal control theory was presented and a new algorithm for weight matrix elements calculation was introduced. The field oriented control of the permanent magnet hysteresis motor has been also proposed to control the hunting.

Time-displacement errors and hunting oscillations have been shown to be reducible when damping is added. Simulation results show that the proposed control strategy is efficient and provides a good performance and reduces the hunting excursion significantly.

References

[1] Rahman M. A., Qin R., "Starting and Synchronization of Permanent Magnet Hysteresis Motors," *IEEE Transactions on Industry Applications*, Vol. 32, No. 5, pp. 1183-1189, Sep.-Oct. 1996.

[2] Qin R., Rahman M. A, "Magnetic Equivalent Circuit of PM Hysteresis Synchronous Motor," *IEEE Trans. on Magnetics*, Vol. 39, No. 5, pp 2998-3000, Sep. 2003.

[3] Qian J., Rahman M. A.,"Analysis of Field Oriented Control for Permanent Magnet Hysteresis Synchronous Motors," *IEEE Trans. on Industry Applications*, Vol. 29, No. 6, Nov./Dec. 1993.

[4] Rahman M. A., Osheiba A. M., Little T. A., Slemon G. R., "Effects of samarium cobalt permanent magnet on the performance of polyphase hysteresis-reluctance motors," *IEEE Trans. Magn*., Vol. MAG-20, pt. 2, pp. 1765-1767, Sep. 1984.

[5] Clurman S. P., "On Hunting in Hysteresis Motors and New Damping Techniques,"*IEEE Trans. Magnetics,* pp. 512-517, Sept. 1971.

[6] Truong C. K., "*Analysis of Hunting in Synchronous Hysteresis Motor,"* thesis on the Degrees of Master of Engineering in Electrical Engineering and Computer Science at the Massachusetts Institute of Technology February 2004.

[7] Khaki-Sedigh A., "*Modern Control Systems*", 3rd edition, Tehran university press, Iran, pp. 267-268, 1996 (in Persian).

[8] Kataoka T., Ishikawa T., and Takahashi T., "Analysis of a hysteresis motor with overexcitation," *IEEE Trans. Magnet.*, Vol. MAG-18, No. 6, pp. 1731-1733, Nov. 1982.

[9] Rahman M. A., "Analytical models for polyphase hysteresis motor," *IEEE Trans. Power App. Syst.*, Vol. PAS-92, No. 1, pp. 237-242, Jan./Feb. 1973.

[10] Rahman M. A., Qin R., "A Permanent Magnet Hysteresis Hybrid Synchronous Motor for Electric Vehicles", *IEEE Trans. Industrial Electronics,* Vol. 44, No. 1, pp. 46-53, Feb. 1997.

[11] Rahman M. A., Osheiba A., "Dynamic Performance Prediction of Polyphase Hysteresis Motors," *IEEE Trans. Industry Applications*, vol. 26, No 6. pp. 1026-1023, Nov./Dec. 1990.
[12] Kurihara K., Rahman M. A., "Transient Performance Analysis for Permanent-Magnet Hysteresis Synchronous Motor," *IEEE Trans. Industry Applications*, Vol. 40, No. 1, pp. 135-142, Jan./Feb. 2004.
[13] Tao-nan Y., *Electric power system dynamics*, Academic Press, Inc., New York, pp. 101-112, 1963.

Appendix

In the [1] a standard stator frame which was initially designed for a 3-phase Mawdsley generalized machine rated at 208-V, 60-Hz, delta-connected in 4-pole, has been employed. The hysteresis material is made of 36% cobalt-steel alloys and the neodymium boron iron (Nd.B.Fe) permanent magnets are arranged within the hysteresis material.
Machine dimensions and design data are given in Table I [1]. The pertinent properties of the rotor materials are given in Table II [1]. And the parameters of the experimental PMHS motor are given in Table III [1].

Table I Design dimensions and data of experimental PMHS motor [1].

Stator		Rotor	
Stator inner diameter	151 mm	Rotor outer diameter	150 mm
Core length	105 mm	Length of rotor ring	105 mm
Number of slots	48	Hysteresis ring thickness	16 mm
Number of poles	4	Air gap length	0.33 mm
Number of turns/coil	27	PM material thickness	6.25 mm
Number of coils	48	Width of PM materials	40 mm
Stator coil pitch	1-13		
Winding factor	0.829		
Type of winding	Double layer lap.		

Table II Properties of hysteresis and permanent magnet materials [1].

Properties	Materials	
	36% Cobalt steel	Nd.B.Fe
Hysteresis loss (kJ/cycle/m^3)	90.0	-
Residual flux density (T)	0.96	1.14
Coercive force (kA/m)	19.09	862.37
Energy product (kJ/m^3)	7.96	247.49
Recoil permeability	18.00	1.01

Table III The parameters of the experimental PMHS motor [1].

Parameters	Values
Stator leakage inductance (H)	0.0086
Rotor leakage inductance (H)	0.0070
Hysteresis incremental inductance (H)	0.0050
Rotor hysteresis resistance (Ω)	9.80
Rotor eddy current resistance (Ω)	18.7

Zahra Nasiri-Gheidari has received her B.Sc. degrees in Electrical Engineering from the Iran University of Sciences and Technology, Tehran, Iran in 2004. And she received the Master degrees in Electrical Power Engineering from the University of Tehran in Iran in 2006, graduating with First Class Honors in both of them. She is currently director of Electrical machinery Lab. in the Electrical Engineering Department of Sharif University of Technology, Tehran, Iran. Her research interests are design and modeling of electrical machines and drives.

Hamid Lesani received the M.Sc. degree in electrical power engineering from the University of Tehran, Iran, in 1975, and the Ph.D. degree in electrical engineering from the university of Dundee, U.K., in 1987. early in his career, he served as a Faculty Member with Mazandaran University. After obtaining the Ph.D. degree, he joined the school of electrical and computer Engineering, Faculty of Engineering, University of Tehran, where he is a professor. His teaching and research interests are design and modeling of electrical machines and power systems. Dr. Lesani is a member of IEEE, and a member of control and intelligent processing center of Excellency, University of Tehran, Iran.

Farid Tootoonchian has received his B.Sc. and M.Sc. degrees in Electrical Engineering from the Iran University of Sciences and Technology, Tehran, Iran in 2000 & 2007 respectively. He has done over 21 industrial projects including one national project about electrical machines over the years, and holds 5 patents. His research interest is design of small electromagnetic machines and sensors.